

Cite this: *CrystEngComm*, 2011, **13**, 293

www.rsc.org/crystengcomm

PAPER

N-Heterocyclic carbene copper(II), mercury(II) and silver(I) complexes containing durene linker: synthesis and structural studies†

Qing-Xiang Liu,* Ai-Hui Chen, Xiao-Jun Zhao, Yan Zang, Xiu-Mei Wu, Xiu-Guang Wang and Jian-Hua Guo

Received 28th April 2010, Accepted 8th July 2010

DOI: 10.1039/c0ce00142b

The dibenzimidazolium salts bis[*N*-(alkyl)benzimidazoliumylmethyl]durene·2X (**1a**: alkyl = C₂H₅, X = Br; **1b**: alkyl = C₂H₅, X = PF₆; **1c**: alkyl = *n*-C₃H₇, X = Cl; **1d**: alkyl = *n*-C₄H₉, X = I; **1e**: alkyl = 1-PyCH₂, X = Br; durene = 1,2,4,5-tetramethylbenzene) and the diimidazolium salt bis-*N*-(butyl)imidazoliumylmethyl]durene hexafluorophosphate (**1f**), and their seven NHC copper(II), mercury(II) and silver(I) complexes, [durene(CH₂bimyEt)₂Cu₂I₂] (**2b**), [durene(CH₂bimyEt)₂HgBr]·0.5[HgBr₄] (**2c**), [durene(CH₂bimy^{''}Bu)₂Hg₂(CHCN)][HgI₄] (**2d**), [durene(CH₂imy^{''}Bu)₂Ag₂(CH₂CN)₂] (**2e**), [durene(CH₂bimyPyCH₂)₂Ag₂Br₂] (**2f**), [durene(CH₂bimyEt)₂Ag][PF₆] (**2g**) and [durene(CH₂bimy^{''}Bu)₂Ag₂(OH)₂] (**2h**), as well as one anionic complex [durene(CH₂benzimidazoliumyl^{''}Pr)₂][PdCl₃(DMSO)]₂ (**2a**) (bimy = benzimidazol-2-ylidene, imy = imidazol-2-ylidene), have been prepared and characterized. These compounds adopt two diverse conformations (*i.e.*, *cis*- and *trans*-conformations). In **2d** and **2e**, an interesting phenomenon is that the α-carbon atoms of deprotonated acetonitrile ([CHCN]²⁻ for **2d** and [CH₂CN]⁻ for **2e**) participate in coordination with metal ions. In the crystal packings of these complexes, 1D supramolecular chains or 2D supramolecular layers are formed *via* intermolecular weak interactions, including π–π interactions, hydrogen bonds and C–H⋯π contacts.

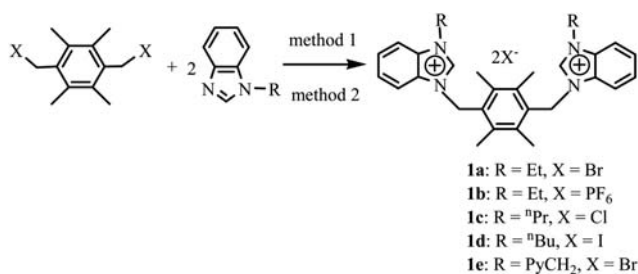
Introduction

N-Heterocyclic carbenes (NHCs) have received a burst of attention as new ligands since the isolation of the first free stable *N*-heterocyclic carbenes by Arduengo and coworkers.¹ A variety of relevant metal complexes have been synthesized through deprotonation of *N,N'*-disubstituted benzimidazolium (or imidazolium) salts.² Strong electron-donating ability of NHC ligands leads to their metal complexes of high stability to heat, moisture and air.³ NHC-metal complexes have shown to be efficient catalysts for some organic reactions, such as Heck, Suzuki and Kumada couplings, and olefin metathesis.⁴ Of known NHC-metal complexes, the NHC copper(II),⁵ mercury(II)⁶ and silver(I)⁷ complexes have played important roles in the development of *N*-heterocyclic carbene chemistry. Particularly, *N*-heterocyclic carbene silver(I) complexes can be used as carbene transfer reagents for the synthesis of Ni, Pd, Pt, Cu, Au, Rh, Ir and Ru carbene complexes, which affords a convenient method for the preparation of these metal carbene complexes.⁸

In the family of NHCs, a number of functional bidentate bis-NHC ligands and their metal complexes have been studied. Among these bidentate bis-NHC ligands, a pair of NHC moieties are connected by a bridging linker, such as alkyl,⁹ aryl,¹⁰ pyridinediyl¹¹ and ether chain.¹² This type of ligand along with metal ions readily form cyclic NHC-metal complexes, which may have potential application in organic reactions as catalyst and in molecular recognition as an acceptor. We are interested in bidentate bis-NHC ligands and their metal complexes. Recently, some silver(I) and mercury(II) complexes based on bidentate bis-NHC ligands with alkyl or oligoether linkers have been reported by us.¹³ We report herein the synthesis, structures and fluorescent emission spectra of NHC-metal complexes containing durene linker, [durene(CH₂bimyEt)₂Cu₂I₂] (**2b**), [durene(CH₂bimyEt)₂HgBr]·0.5[HgBr₄] (**2c**), [durene(CH₂bimy^{''}Bu)₂Hg₂(CHCN)][HgI₄] (**2d**), [durene(CH₂imy^{''}Bu)₂Ag₂(CH₂CN)₂] (**2e**), [durene(CH₂bimyPyCH₂)₂Ag₂Br₂] (**2f**), [durene(CH₂bimyEt)₂Ag][PF₆] (**2g**) and [durene(CH₂bimy^{''}Bu)₂Ag₂(OH)₂] (**2h**), and one anionic complex [durene(CH₂benzimidazoliumyl^{''}Pr)₂][PdCl₃(DMSO)]₂ (**2a**) (bimy = benzimidazol-2-ylidene, imy = imidazol-2-ylidene, durene = 1,2,4,5-tetramethylbenzene) is also described in the paper. In addition, we also report two diverse conformations (*i.e.*, *cis*- and *trans*-conformations) of the dibenzimidazolium salts and their metal complexes. Moreover, the α-carbon atoms of deprotonated acetonitrile in **2d** and **2e** participate in

Tianjin Key Laboratory of Structure and Performance for Functional Molecule, College of Chemistry, Tianjin Normal University, Tianjin, 300387, P. R. China. E-mail: qxliu@eyou.com

† CCDC reference numbers 757348–757355 and 775637. For crystallographic data in CIF or other electronic format see DOI: 10.1039/c0ce00142b



Reagents: method 1 for **1a**, **1c** and **1e**, THF, reflux.
 method 2 for **1b** and **1d**, (i) THF, reflux; (ii) anionic exchange with NH₄PF₆ in methanol for **1b**, and with NaI in acetone for **1d**.

Scheme 1 Preparation of precursors **1a–1e**.

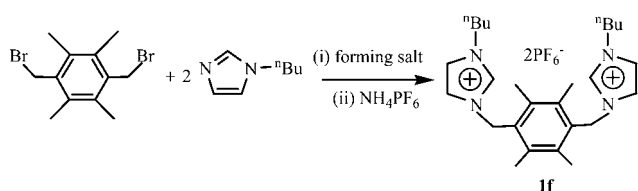
coordination with metal ions, and this observation is also interesting in organometallic chemistry.

Results and discussion

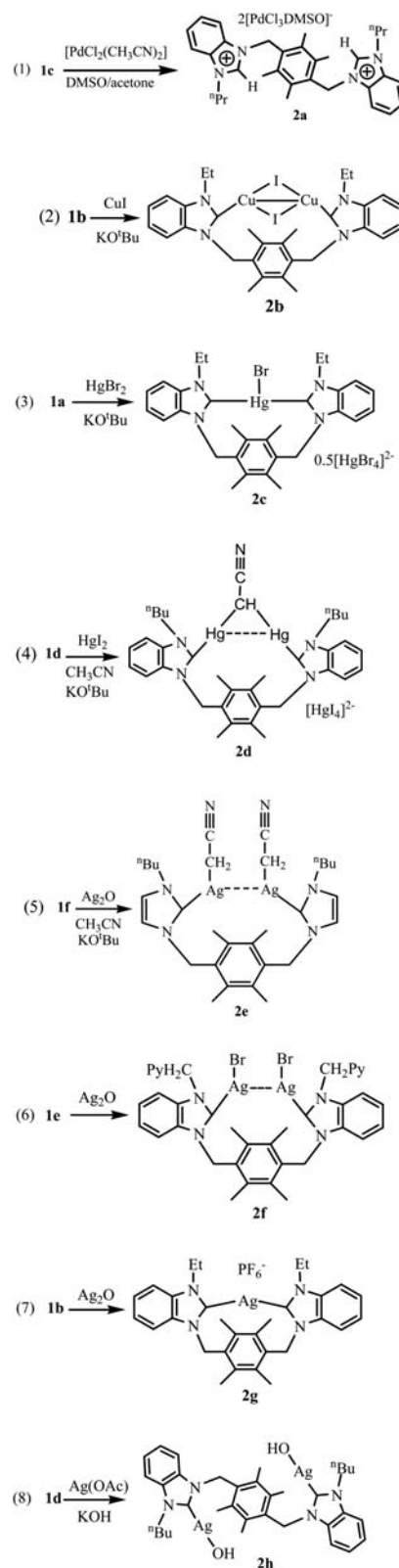
Synthesis and general characterization of precursors **1a–1f** and complexes **2a–2h**

The dibenzimidazolium salts, bis[*N*-(alkyl)benzimidazolium]methyl]durene halogenide (**1a**: alkyl = Et, halogenide = Br; **1c**: alkyl = ⁿPr, halogenide = Cl; **1e**: alkyl = 1-PyCH₂, halogenide = Br) were prepared from benzimidazole by alkylation with 1-bromoethane or 2-chloromethylpyridine followed by quarterization with bis-(bromomethyl)durene in sequence (method 1, Scheme 1). The bis[*N*-(ethyl)benzimidazolium]methyl]durene hexafluorophosphate (**1b**) and the bis[*N*-(*n*-butyl)benzimidazolium]methyl]durene iodide (**1d**) were obtained in two steps. The first step is in a manner similar to that of **1a**, and the second step is through an anionic exchange with ammonium hexafluorophosphate in methanol for **1b** and with sodium iodide in acetone for **1d** (method 2, Scheme 1). The diimidazolium salt bis[*N*-(*n*-butyl)imidazolium]methyl]durene hexafluorophosphate (**1f**) was prepared in a manner similar to that for **1b** (Scheme 2). Precursors **1a–1f** are stable towards air and moisture, soluble in polar organic solvents such as dichloromethane, acetonitrile and methanol, and scarcely soluble in benzene, diethyl ether and petroleum ether. In the ¹H NMR spectra of **1a–1f**, the benzimidazolium (or imidazolium) proton signals (NCHN) appear at δ = 9.90–10.60 ppm, which are consistent with the chemical shifts of reported benzimidazolium (or imidazolium) salts.²

Synthetic methods of complexes **2a–2h** are shown in Scheme 3. The reaction of **1c** with [PdCl₂(CH₃CN)₂] afford an anionic complex [durene(CH₂benzimidazoliumylⁿPr)₂][PdCl₃(DMSO)]₂ (**2a**) (Scheme 3(1)). **1b** was treated with copper(i) iodide and silver oxide, respectively, to afford complexes [durene-(CH₂bimyEt)₂Cu₂I₂] (**2b**) and [durene(CH₂bimyEt)₂Ag][PF₆]



Scheme 2 Preparation of precursor **1f**.



Scheme 3 Preparation of complexes **2a–2h**.

(**2g**) (Scheme 3(2) and (7)). Complex [durene(CH₂bimyEt)₂HgBr][0.5[ⁿHgBr₄]] (**2c**) was prepared by the reaction of **1a** with anhydrous mercury(II) bromide (Scheme 3(3)). **1d** was treated with anhydrous mercury(II) iodide and silver

acetate, respectively, to afford complexes [durene-(CH₂bimyⁿBu)₂Hg₂(CHCN)][HgI₄] (**2d**) and [durene(CH₂bimyⁿBu)₂Ag₂(OH)₂] (**2h**) (Scheme 3(4) and (8)). Complex [durene(CH₂bimyⁿBu)₂Ag₂(CH₂CN)₂] (**2e**) was prepared *via* reaction of **1f** with silver oxide (Scheme 3(5)). Complex [durene(CH₂bimyPyCH₂)₂Ag₂Br₂] (**2f**) was prepared *via* reaction of **1e** with silver oxide (Scheme 3 (6)). Complexes **2a–2h** are stable towards air and moisture, soluble in DMSO and insoluble in diethyl ether and hydrocarbon solvents. In the ¹H NMR spectra of **2b–2h**, the disappearance of the resonances for the benzimidazolium (or imidazolium) protons (NCHN) shows the formation of the expected metal carbene complexes, and the chemical shifts of other hydrogens are similar to those of corresponding precursors. The ¹H NMR spectrum of anionic complex **2a** is similar to that of corresponding precursor **1c**. In ¹³C NMR spectra, the signals for the carbene carbon of **2b–2d** and **2f–2h** appear at 174.4–187.3 ppm, which are similar to known metal carbene complexes.^{5–7} The signal of carbene carbon in **2e** was not observed. Similar results have been reported for some carbene-silver(i) complexes, which may result from the fluxional behavior of the NHC complexes.¹⁴ For complexes **2d** and **2e** containing deprotonated acetonitriles, the signals of carbon of cyano group (CN) appear at 113.4 ppm for **2d** and 112.7 ppm for **2e**, and the signals of α-carbon atom of acetonitrile appear at 30.3 ppm for **2d** and 31.2 ppm for **2e**. IR spectra contain the characteristic bands of cyano groups at 2191 cm^{−1} for **2d** and 2166 cm^{−1} for **2e**. These values are comparable to those of the reported complexes containing cyano groups.¹⁵

Structures of dibenzimidazolium salt **1e** and complexes **2a–2h**

Molecular structures of precursor **1e** and complexes **2a–2h** were demonstrated by X-ray analysis. The crystals of **1e**·CH₃CN, **2a**, **2b**·0.5CH₃CN, **2c**·0.5DMSO, **2d**·CH₃CN, **2e**, **2f**·DMSO, **2g**·0.5H₂O and **2h** suitable for X-ray diffraction were obtained by slow diffusion of diethyl ether into their DMSO/CH₃CN solution. In complexes **2c** and **2g**, each cation contains a mononuclear macrometallocycle formed by one bidentate chelate carbene ligand and one metal atom, whereas complexes **2b**, **2d**, **2e** and **2f** possess dinuclear macrometallo-cyclic structures as shown in Fig. 1(a), Fig. 2(a) and Fig. 6(a)–Fig. 9(a). In each of **1e** and **2b–2g**, two Rbimi (or Rimi) arms lie in the same side of durene plane to adopt a *cis*-conformation. The two benzimidazole (or imidazole) rings within each molecule form the dihedral angles varying from 5.1° to 56.0°, and they form the dihedral angles in the ranges of 76.4–91.9° and 81.7–96.9° with the centric durene

Table 1 Dihedral angles (°) between two benzimidazole (or imidazole) rings (A), and dihedral angles (°) between two benzimidazole (or imidazole) rings and durene plane (B) for precursor **1e** and complexes **2b–2g**

Compounds	A	B
1e	9.5(1)	86.4(1), 81.8(1)
2b	5.1(3)	82.0(2), 86.4(1)
2c	6.6(1)	88.1(1), 84.3(4)
2d	56.0(2)	76.4(2), 81.7(1)
2e	9.0(1)	81.7(1), 90.5(1)
2f	6.4(2)	91.9(2), 92.9(3)
2g	18.6(1)	78.7(1), 96.9(2)

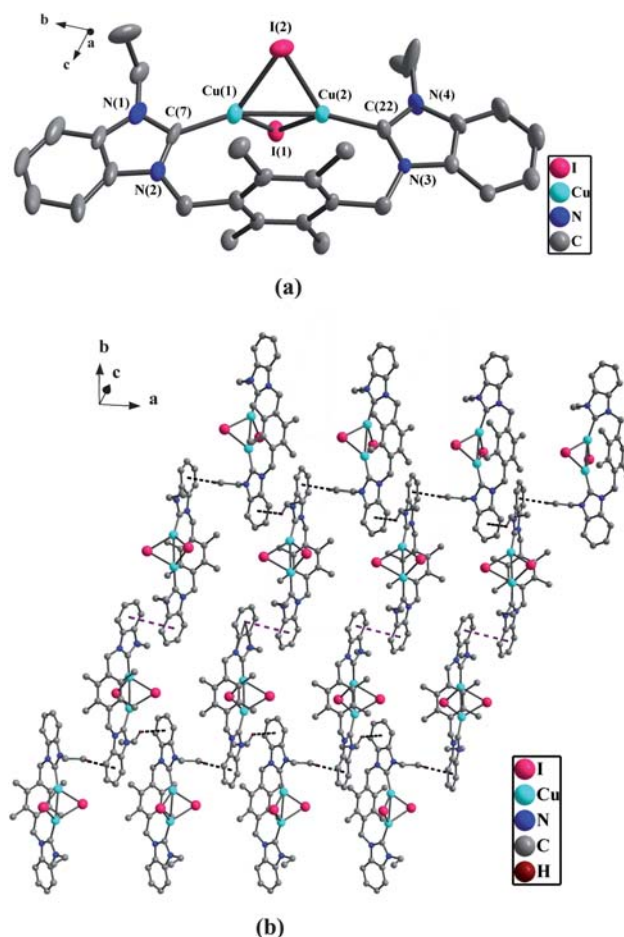


Fig. 1 (a) Perspective view of **2b** and anisotropic displacement parameters depicting 30% probability. All hydrogen atoms were omitted for clarity. Selected bond lengths (Å) and angles (°): Cu(1)–I(1) 2.660(1), Cu(1)–I(2) 2.600(1), Cu(1)–Cu(2) 2.668(1); I(1)–Cu(1)–Cu(2) 57.8(4), N(1)–C(7)–N(2) 106.7(7), N(3)–C(22)–N(4) 105.6(6). (b) The 2D supramolecular layers by the π – π interactions and C–H \cdots π contacts in **2b**. All hydrogen atoms except those participating in the C–H \cdots π contacts were omitted for clarity.

plane, respectively (the related data being given in Table 1). In contrast, the molecular structures of complexes **2a** and **2h** are different from those of above-mentioned compounds, and two Rbimi arms within each molecule in **2a** and **2h** lie in the opposite sides of durene plane to adopt an open *trans*-conformation as shown in Fig. 3(a) and Fig. 4(a). The X-ray crystal structural analyses of **2a** and **2h** show that there are inversion centers in the complexes. Additionally, two benzimidazole rings within each molecule are parallel, and they form the dihedral angles 82.3(5)° for **2a** and 88.8(2)° for **2h** with the centric durene plane, respectively. In **2b–2h**, the internal ring angles (N–C–N) at the carbene centers are in the range of 102.8–107.5°, which are comparable to those of the known NHC-metal complexes,² but these values are smaller than the corresponding values (110.9–111.1°) of precursor **1e** and anionic complex **2a**.

In precursor **1e**, one bromine atom and four hydrogen atoms on two PyCH₂bimi arms form four C–H \cdots Br hydrogen bonds¹⁶ as shown in Fig. 5(a) (the data of hydrogen bonds being given in Table 2). Anionic complex **2a** is different from precursor **1e**, one

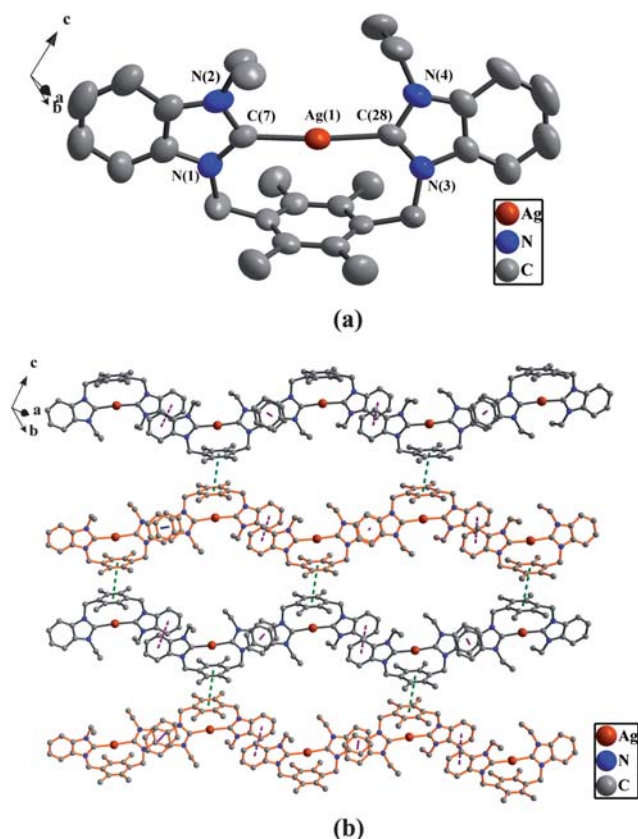


Fig. 2 (a) Perspective view of **2g** and anisotropic displacement parameters depicting 30% probability. All hydrogen atoms and anions $2PF_6^-$ were omitted for clarity. Selected bond lengths (Å) and angles ($^\circ$): Ag(1)–C(7) 2.121(2), Ag(1)–C(28) 2.100(2); N(1)–C(7)–N(2) 105.5(4), N(3)–C(28)–N(4) 106.1(4). (b) The 2D supramolecular layers by the both types of π – π interactions in **2g**. All hydrogen atoms were omitted for clarity.

oxygen atom from DMSO of anionic $[PdCl_3(DMSO)]$ and two hydrogen atoms on one "Prbimi arm in **2a** form two C–H \cdots O hydrogen bonds¹⁷ as shown in Fig. 3(a) (Table 2). In anionic unit $[PdCl_3(DMSO)]$, the center Pd is coordinated to three chlorine atoms and one sulfur atom of DMSO to adopt a planar square array. The bond distances of Pd–Cl are in the range of 2.328–2.348 Å.

In NHC-copper(i) complex **2b** (Fig. 1(a)), each copper(i) atom is tetra-coordinated with one carbene carbon atom (C(carbene)), two iodine atoms and another copper(i) atom. Two copper(i) atoms are linked by two bridging iodine atoms to form a distorted Cu_2I_2 quadrangular arrangement. In the Cu_2I_2 core, the dihedral angle between the Cu(1)–I(1)–Cu(2) plane and Cu(1)–I(2)–Cu(2) plane is $44.3(1)^\circ$. The Cu(1)–Cu(2) distance of 2.668(1) Å (van der Waals radii of copper = 1.86 Å) indicates a strong metal–metal interaction.¹⁸ The bond angles of two Cu–I–Cu are $61.3(4)^\circ$ and $61.5(3)^\circ$. The Cu–I distance of 2.57–2.66 Å falls in the regular range.¹⁹ Additionally, the distances of two Cu–C bonds are 1.962(8) Å and 1.929(1) Å, and the bond angles of two C–Cu–Cu are $159.4(3)^\circ$ and $161.5(1)^\circ$. These values are comparable to those of the reported NHC copper(i) complexes.⁸

In two NHC-mercury(II) complexes **2c** and **2d** (Fig. 6(a) and Fig. 7(a)), the bond distances of Hg–C(carbene) vary from

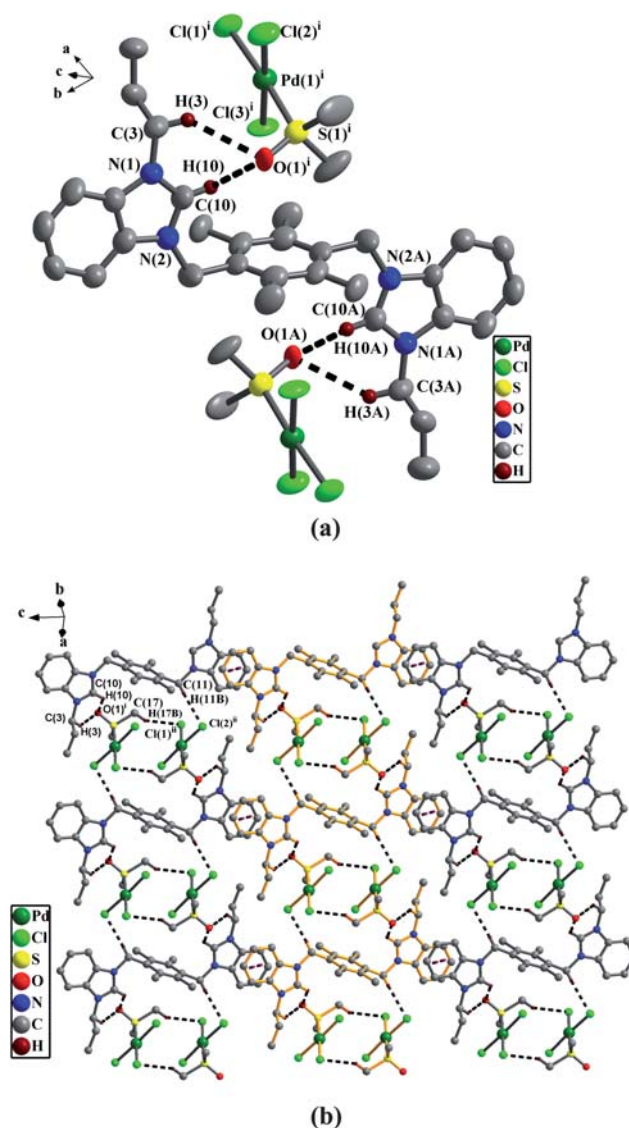


Fig. 3 (a) Perspective view of **2a** and anisotropic displacement parameters depicting 30% probability. All hydrogen atoms except those participating in the C–H \cdots O hydrogen bonds were omitted for clarity. Selected bond lengths (Å) and angles ($^\circ$): N(1)–C(10) 1.332(8), Pd(1)–S(1) 2.239(1), Pd(1)–Cl(1) 2.341(1), Pd(1)–Cl(2) 2.328(1), Pd(1)–Cl(3) 2.348(1); Cl(1)–Pd(1)–Cl(2) $92.1(6)^\circ$, Cl(1)–Pd(1)–Cl(3) $89.0(6)^\circ$, Cl(2)–Pd(1)–Cl(3) $176.9(7)^\circ$, S(1)–Pd(1)–Cl(2) $88.6(6)^\circ$, S(1)–Pd(1)–Cl(3) $90.2(6)^\circ$, N(1)–C(10)–N(2) $111.0(6)^\circ$. (b) The 2D supramolecular layers by the π – π interactions, C–H \cdots O hydrogen bonds and C–H \cdots Cl hydrogen bonds in **2a**. All hydrogen atoms except those participating in the hydrogen bonds were omitted for clarity.

2.082(8) Å to 2.101(6) Å, which are similar to those of known NHC-mercury(II) complexes.⁶ The anionic units of **2c** and **2d** are tetrahedral $[HgBr_4]^{2-}$ and $[HgI_4]^{2-}$, respectively, in which the values of bond lengths and bond angles fall in regular range.²⁰ In **2c**, the mercury(II) atom within the cationic macrometallocycle is tri-coordinated with two carbene carbons and one bromine atom. The C(1)–Hg(1)–C(22) array is nearly linear with the bond angle of $173.7(3)^\circ$. The two ethyl chains and one bromine atom in the cation are stretching in the same direction. In the cationic unit of **2d**, the Hg(2) and Hg(3) are dicoordinated with one

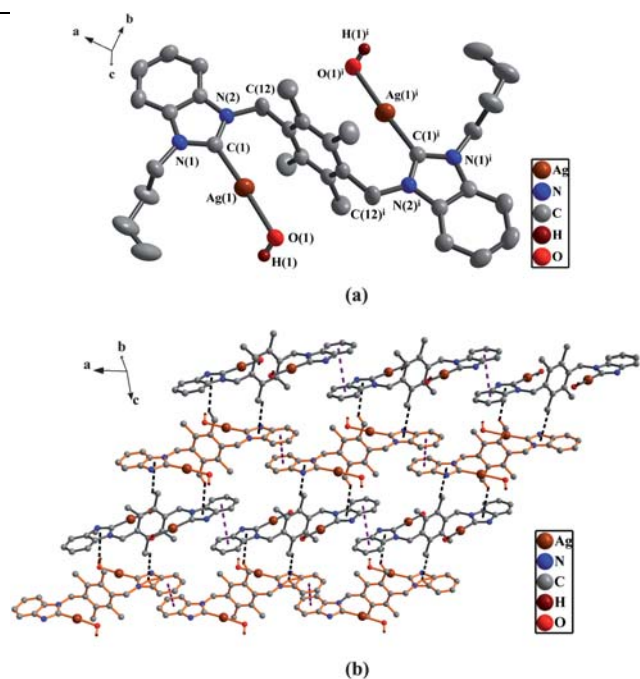


Fig. 4 (a) Perspective view of **2h** and anisotropic displacement parameters depicting 30% probability. All hydrogen atoms except those in the OH were omitted for clarity. Selected bond lengths (Å) and angles (°): Ag(1A)–C(1A) 2.101(3), O(1A)–H(1A) 0.820(1); N(1A)–C(1A)–N(2A) 105.7(3). (b) The 2D supramolecular layers by the π – π interactions and C–H... π contacts in **2h**. All hydrogen atoms except those participating in the C–H... π contacts and in the OH, and all butyl groups on the nitrogen atoms were omitted for clarity.

carbene carbon atom and one α -carbon atom (C(α)) of deprotonated acetonitrile. The bond distances of two Hg–C(carbene) (2.082(8) Å and 2.084(8) Å) are slightly shorter than those of Hg–C(α) (2.090(8) Å and 2.112(8) Å). The Hg(2)...Hg(3) separation of 3.338(5) Å (van der Waals Radii of mercury = 1.70 Å) indicates a weak metal–metal interaction.²⁰ Two C(carbene)–Hg–C(α) arrays are nearly linear with the bond angles of 172.8(4)° and 176.9(3)°. The bond angles of two Hg–C(35)–C(36) are 113.5(6)° and 114.7(7)°, and the bond angle of Hg(2)–C(35)–Hg(3) is 105.2(3)°. Notably, the cyanomethyl moiety (C(35)–C(36)–N(5)) is nearly linear with a bond angle of 177.9(1)°. The C(35)–C(36) bond distance (1.398(1) Å) is shorter than that of the regular C–C single bond (1.54–1.59 Å), and it has partial double-bond character. The C(36)–N(5) bond distance (1.167(1) Å) is similar to that of other complexes containing cyano groups, and this value is expected for a triple bond with a small amount of double bond character.²¹ The two butyl chains on the nitrogen atoms are stretching in the opposite directions.

In four NHC-silver(I) complexes **2e–2h**, each silver(I) atom possesses a dicoordinated geometry, and the bond distances of Ag–C(carbene) vary from 2.058(7) Å to 2.121(2) Å. These values are comparable to known NHC-silver(I) complexes.⁵ As for **2e**, the data of all bond lengths and angles in the [CH₂CN][–] unit are comparable to the corresponding values in [CHCN]^{2–} unit of **2d**. The two C(carbene)–Ag–C(α) arrays are nearly linear with the bond angles of 173.0(3)° and 173.6(3)°. The bond distances of two Ag–C(carbene) (2.058(7) Å and 2.066(7) Å) are slightly

Table 2 H-Bonding geometry (Å, °) for **1e**, **2a**, **2d** and **2e**^a

	D–H...A	D–H	H...A	D...A	D–H...A
1e	C(6)–H(6A)...Br(2)	0.97(4)	2.781(5)	3.654(3)	150.0(2)
	C(13)–H(13)...Br(2)	0.93(3)	2.814(5)	3.572(4)	139.4(2)
	C(33)–H(33B)...Br(2)	0.97(4)	3.135(6)	3.974(4)	145.5(2)
	C(32)–H(32)...Br(2)	0.93(3)	3.155(7)	3.723(4)	121.2(4)
2a	C(3)–H(3)...O(1) ⁱ	0.97(8)	2.668(8)	3.463(1)	139.4(4)
	C(10)–H(10)...O(1) ⁱ	0.93(7)	2.679(8)	3.227(1)	118.4(4)
	C(11)–H(11B)...Cl(2) ⁱⁱ	0.97(8)	2.721(1)	3.608(7)	152.3(5)
	C(17)–H(17B)...Cl(1) ⁱⁱ	0.96(9)	2.829(2)	3.518(1)	129.5(6)
2d	C(35)–H(35)...I(1) ⁱ	0.98(1)	3.189(1)	3.923(3)	133.1(1)
	C(12)–H(12)...I(4)	0.97(1)	3.010(2)	3.689(1)	128.0(3)
2e	C(21)–H(21)...N(6) ⁱ	0.93(1)	2.334(1)	3.219(1)	158.9(3)

^a Symmetry code: *i* = 1 – *x*, 1 – *y*, 1 – *z*; *ii* = –1 + *x*, 2 + *y*, 2 + *z* for **2a**. *i* = *x*, –1 + *y*, *z* for **2d**. *i* = 1 + *x*, *y*, *z* for **2e**.

longer than those of two Ag–C(α) (1.913(1) Å and 1.975(7) Å). The Ag...Ag separation of 3.304(1) Å (van der Waals Radii of silver = 1.72 Å) indicates a weak metal–metal interaction.²² The two *n*-butyl groups on the nitrogen atoms are stretching in the

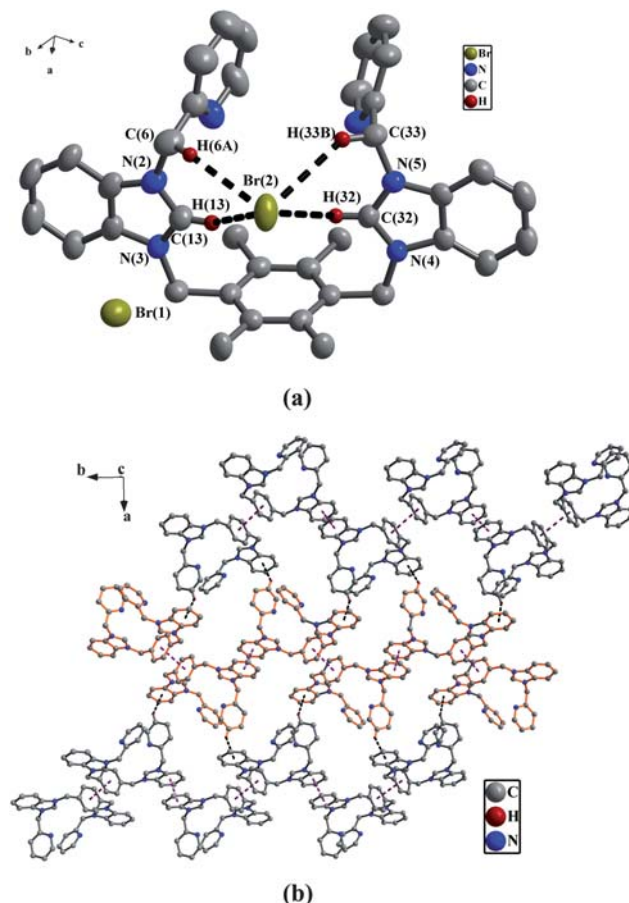


Fig. 5 (a) Perspective view of **1e** and anisotropic displacement parameters depicting 30% probability. All hydrogen atoms except those participating in the C–H...Br hydrogen bonds were omitted for clarity. Selected bond lengths (Å) and angles (°): C(13)–N(2) 1.317(4); N(2)–C(13)–N(3) 111.1(3), N(4)–C(32)–N(5) 110.9(2). (b) The 2D supramolecular layers by the π – π interactions and C–H... π contacts in **1e**. All hydrogen atoms except those participating in the C–H... π contacts, all methyl groups on the durenes and all bromine atoms were omitted for clarity.

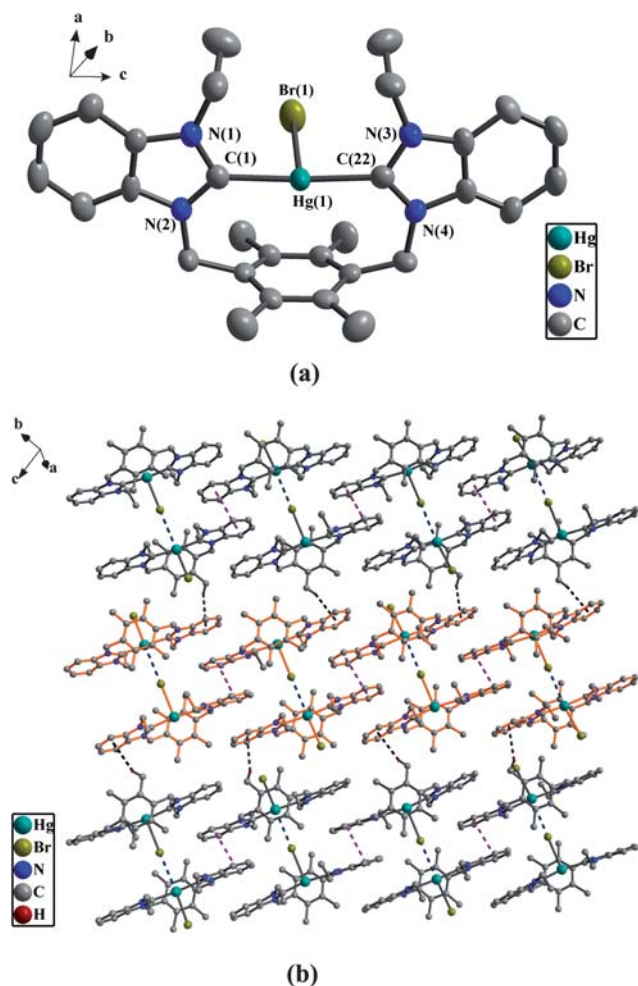


Fig. 6 (a) Perspective view of **2c** and anisotropic displacement parameters depicting 30% probability. All hydrogen atoms and anion $0.5[\text{HgBr}_4]^{2-}$ were omitted for clarity. Selected bond lengths (Å) and angles ($^\circ$): Hg(1)–C(1) 2.097(6), Hg(1)–Br(1) 3.076(1); C(1)–Hg(1)–C(22) 173.7(3), C(1)–Hg(1)–Br(1) 90.4(2), N(1)–C(1)–N(2) 107.5(5), N(3)–C(22)–N(4) 108.2(6). (b) The 2D supramolecular layers by the weak Hg \cdots Br bonds, π – π interactions and C–H \cdots π contacts in **2c**. All hydrogen atoms except those participating in the C–H \cdots π contacts were omitted for clarity.

same direction, whereas the two $[\text{CH}_2\text{CN}]^-$ units are stretching in the opposite directions.

The macrometallocycle of **2f** is analogous to that of **2e**, however, the Ag \cdots Ag separation of 3.113(7) Å in **2f** is shorter than that of 3.304(1) Å in **2e**. The bond distances of two Ag–Br in **2f** are 2.492(6) Å and 2.437(7) Å, and the bond angles of two C–Ag–Br are 159.6(1) $^\circ$ and 166.9(1) $^\circ$. The two bromine atoms are stretching in the opposite directions. The dihedral angle between pyridine ring and adjacent benzimidazole is 88.2(1) $^\circ$ (73.3(1) $^\circ$ for the corresponding precursor **1e**), and the dihedral angle between two pyridine rings is 64.3(1) $^\circ$ (37.5(2) $^\circ$ for **1e**). Compared to **1e**, some relevant bond lengths and angles of complex **2f** occur relatively large changes due to the introduction of metal silver(I) atom. As for **2g**, the C(7)–Ag(1)–C(28) array is almost linear with the bond angle of 175.8(6) $^\circ$. The two ethyl chains on the nitrogen atoms are stretching in the opposite directions.

In the *trans* structure of **2h**, the hydroxy groups linked on silver(I) atoms come from KOH. Two $[\text{Bubim}(\text{Ag}(\text{OH}))]$ units are

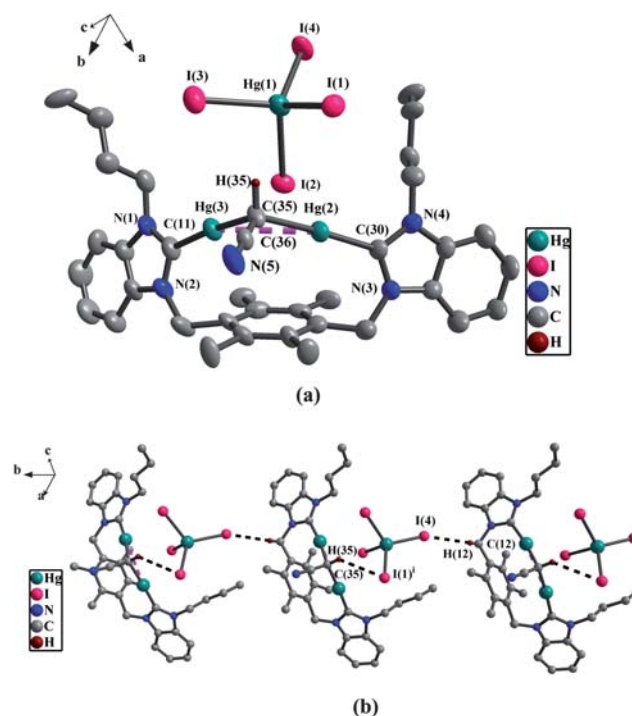
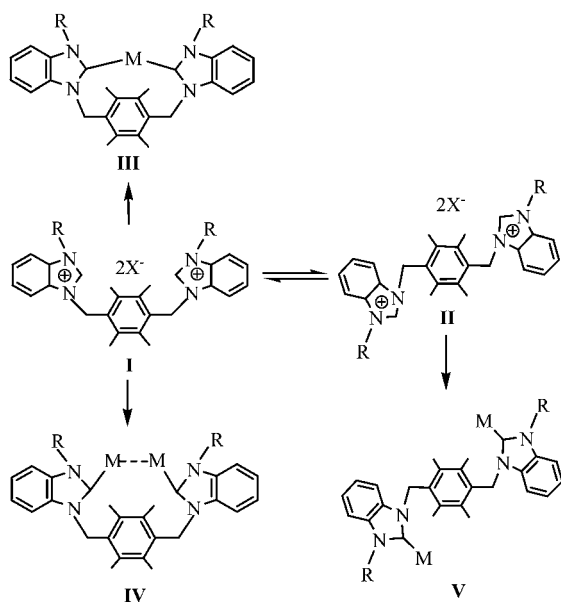


Fig. 7 (a) Perspective view of **2d** and anisotropic displacement parameters depicting 30% probability. All hydrogen atoms except that in the $[\text{CHCN}]^{2-}$ were omitted for clarity. Selected bond lengths (Å) and angles ($^\circ$): N(5)–C(36) 1.167(1), C(35)–C(36) 1.398(1), Hg(3)–C(11) 2.084(8); N(5)–C(36)–C(35) 177.9(1), C(30)–Hg(2)–C(35) 176.9(3), C(36)–C(35)–Hg(3) 113.5(6), C(36)–C(35)–Hg(2) 114.7(7), N(1)–C(11)–N(2) 107.5(7), N(3)–C(30)–N(4) 106.9(7). (b) The 1D supramolecular chains by the C–H \cdots I hydrogen bonds in **2d**. All hydrogen atoms except those participating in the C–H \cdots I hydrogen bonds were omitted for clarity.

placed in the opposite sides of the durene plane. An *n*-butyl group and a AgOH part on same benzimidazole ring are stretched along the benzimidazole ring plane in the same direction, but they point to the opposite directions as compared with the corresponding parts on another benzimidazole ring. The angles of two C–Ag–O (177.1(1) $^\circ$) and the bond distances of two Ag–O (2.274(3) Å) are the same, respectively, and they fall into the regular range.²³

The conformations of the dibenzimidazole salts and their metal complexes

As shown in Scheme 4, the dibenzimidazole salts containing durene linker adopt two diverse conformations (*i.e.*, *cis*-conformation **I** and *trans*-conformation **II**) according to the different arrangements of two Rbimi arms. The conformations **I** and **II** can converse each other in the solution, and their ratio are mostly relative to two factors: (1) the weak interactions between anions and two Rbimi arms; (2) the steric hindrance between two Rbimi arms. The former may have larger effect on the ratio of conformation than the latter. When there exist strong interactions between one anion and two Rbimi arms at the same time in a compound, the two arms lie in same side of durene plane, and the compound adopts mainly *cis*-conformation (*e.g.*, **1e**). When there exist strong interactions between one anion and only one Rbimi arm in a compound, the two arms lie in opposite sides of



Scheme 4 The diverse conformations of dibenzimidazole and their metal complexes

durene plane due to steric hindrance, and the compound adopts mainly *trans*-conformation (e.g., **2a**).

Similarly, NHC metal complexes formed *via* dibenzimidazole salts and metal compounds possess both *cis*-conformations **III** or **IV** (e.g., **2b–2g**) and *trans*-conformation **V** (e.g., **2h**), and their conformations may depend mainly on the conformations of the corresponding precursors. Additionally, NHC metal complexes possessing *cis*-conformation have usually two different structures, namely, single nuclear macrocycle complexes **III** (e.g., **2c** and **2g**) and dinuclear macrocycle complexes **IV** (e.g., **2b**, **2d**, **2e** and **2f**). In dinuclear macrocycle complexes, metal–metal interactions are observed.

The different formulae of deprotonated acetonitrile

An interesting phenomenon during the preparation of **2d** or **2e** is that α -hydrogen atoms of acetonitrile are deprotonated due to the presence of strong base KO^tBu to generate doubly

deprotonated acetonitrile ($[\text{CHCN}]^{2-}$) for **2d** and singly deprotonated acetonitrile ($[\text{CH}_2\text{CN}]^-$) for **2e**. The α -carbon atom (C(α)) of these deprotonated acetonitrile along with didentate carbene ligands are coordinated to metal atoms to form complexes **2d** and **2e**, respectively. A distinction is that the α -carbon atom of $[\text{CHCN}]^{2-}$ in **2d** is bonded to two mercury(II), whereas the α -carbon atom of $[\text{CH}_2\text{CN}]^-$ in **2e** is bonded to one silver(I). From the structures of complexes **2d** and **2e**, as well as reported compounds containing deprotonated acetonitrile, such as $(\text{Me}_3\text{Ge})_2\text{CHCN}$,^{21a} $[\text{Pt}(\text{CH}_2\text{CN})(\text{PMe}_2\text{Ph})_3]\text{PF}_6$,^{21b} $\text{PdCl}(\text{CH}_2\text{CN})(\text{PPh}_3)_2$ ^{21c} and $\text{Fe}_3(\text{Cp})_3(\mu\text{-CO})_3[\mu_3\text{-CCN}]$,^{21d} we know that three α -hydrogen atoms of acetonitrile may be deprotonated one by one in the presence of base to form singly, doubly and triply deprotonated acetonitrile (i.e., $[\text{CH}_2\text{CN}]^-$, $[\text{CHCN}]^{2-}$ and $[\text{CCN}]^{3-}$), respectively. The different formulae of deprotonated acetonitriles probably are relative to the amount of base and the type of coordinated metal ions in the system of reaction.

The crystal packings of precursor **1e** and complexes **2a–2h**

Analyses of the crystal packings of **1e** and **2a–2h** reveal that 2D supramolecular layers of **1e**, **2a**, **2b**, **2c** and **2f–2h**, as well as 1D supramolecular chains of **2d** and **2e** are formed *via* intermolecular weak interactions, including π – π stacking interactions, hydrogen bonds, C–H $\cdots\pi$ contacts and weak Hg \cdots Br bonds (the data of hydrogen bonds being given in Table 2, and the related data of π – π interactions and C–H $\cdots\pi$ contacts being given in Table 3).

In **1e**, the intermolecular weak interactions involve the C–H $\cdots\pi$ contacts²⁴ (the hydrogen atoms being from pyridine rings) and two types of aromatic π – π stacking interactions.²⁵ In these two types of π – π interactions, one is from intermolecular benzene rings of durenes, and another is from intermolecular benzimidazole rings (Fig. 5(b)). An interesting feature in the crystal packing of **2a** is that 1D supramolecular chains are formed by the π – π stacking interactions from intermolecular benzimidazole rings. In addition, an anionic dimer with a 12-membered ring $[\text{PdCl}_3(\text{DMSO})]_2^{2-}$ are formed by two anions $[\text{PdCl}_3(\text{DMSO})]^-$ *via* two C–H \cdots Cl hydrogen bonds (C(17)–H(17B) \cdots Cl(1)).²⁶ These anionic dimeric units $([\text{PdCl}_3(\text{DMSO})]_2)$ are packed between the 1D chains to extend 1D chains into 2D supramolecular layers *via* new

Table 3 Distances (Å) of π – π interactions, and distances (Å) and angles (°) of C–H $\cdots\pi$ contacts for **1e**, **2a–2c** and **2e–2h**

Compounds	π – π		C–H $\cdots\pi$	
	Face-to-face	Center-to-center	H $\cdots\pi$	C–H $\cdots\pi$
1e	3.748(3) (benzene) 3.444(2) (benzimidazole)	3.790(1) (benzene) 3.644(2) (benzimidazole)	2.908(2)	138.7(3)
2a	3.651(3) (benzimidazole)	3.440(1) (benzimidazole)	–	–
2b	3.375(2) (benzimidazole)	3.760(3) (benzimidazole)	2.768(2)	119.4(1)
2c	3.393(1) (benzimidazole)	3.564(2) (benzimidazole)	2.968(1)	139.0(4)
2e	3.521(3) (imidazole)	4.424(1) (imidazole)	–	–
2f	3.463(1) (benzimidazole)	3.776(3) (benzimidazole)	3.033(1)	143.7(2)
2g	3.686(2) (benzene) 3.530(4) (benzimidazole)	3.757(1) (benzene) 3.736(1) (benzimidazole)	–	–
2h	3.534(2) (benzimidazole)	3.732(1) (benzimidazole)	3.002(2)	123.7(1)

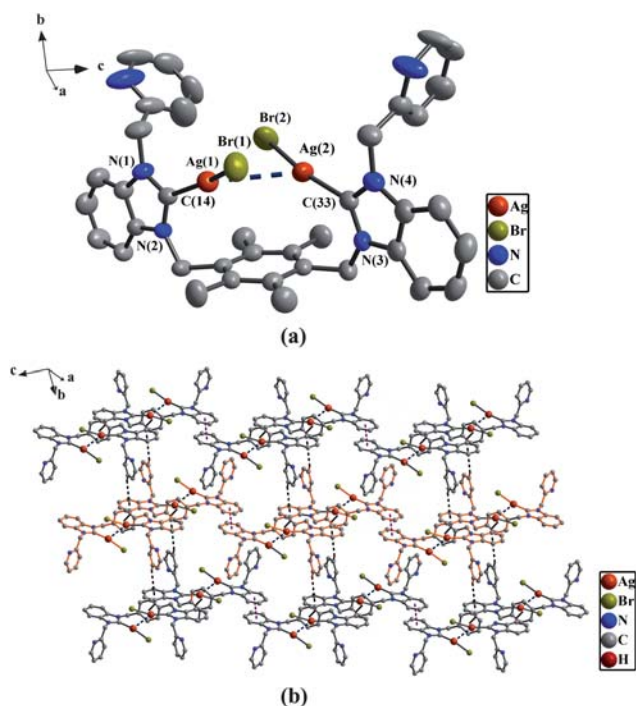


Fig. 8 (a) Perspective view of **2f** and anisotropic displacement parameters depicting 30% probability. All hydrogen atoms were omitted for clarity. Selected bond lengths (Å) and angles (°): Ag(1)–C(14) 2.115(4), Ag(2)–C(33) 2.081(4); C(14)–Ag(1)–Br(1) 159.6(1), C(33)–Ag(2)–Br(2) 166.9 (1), N(1)–C(14)–N(2) 105.2(3). (b) The 2D supramolecular layers by the π – π interactions and C–H \cdots π contacts in **2f**. All hydrogen atoms except those participating in the C–H \cdots π contacts and all methyl groups on the durennes were omitted for clarity.

C–H \cdots Cl hydrogen bonds (C(11)–H(11B) \cdots Cl(2)) as shown in Fig. 3(b).

In **2b**, **2f** and **2h**, there exist the π – π stacking interactions from intermolecular benzimidazole rings and C–H \cdots π contacts (the hydrogen atoms being from ethyl groups on nitrogen atoms for **2b**, from pyridine rings for **2f**, and from methyl groups of durennes for **2h**) (Fig. 1(b) for **2b**, Fig. 8(b) for **2f** and Fig. 4(b) for **2h**). In **2c**, the intermolecular weak interactions include the π – π stacking interactions from intermolecular benzimidazole rings, C–H \cdots π contacts (the hydrogen atoms being from methyl groups of durennes) and weak Hg \cdots Br bonds (Hg \cdots Br distance = 3.602(2) Å)²⁰ (Fig. 6(b)). In **2g**, both types of aromatic π – π stacking interactions are observed (Fig. 2(b)). One type is formed *via* intermolecular benzene rings of durennes, and another is formed *via* intermolecular benzimidazole rings.

Different from the compounds above-mentioned, the adjacent cationic units in **2d** are held together by anionic units [HgI₄]^{2–} *via* C–H \cdots I hydrogen bonds²⁷ to form 1D supramolecular chains (Fig. 7(b)). The double-strand 1D supramolecular chains in **2e** are formed *via* C–H \cdots N hydrogen bonds²⁸ (the hydrogen atoms being from imidazole rings, and nitrogen atoms being from cyano groups) and π – π stacking interactions from intermolecular imidazole rings (Fig. 9(b)).

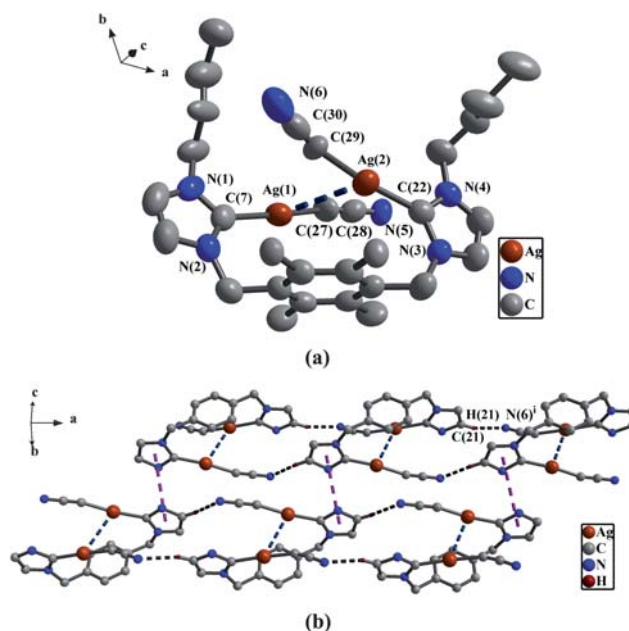


Fig. 9 (a) Perspective view of **2e** and anisotropic displacement parameters depicting 30% probability. All hydrogen atoms were omitted for clarity. Selected bond lengths (Å) and angles (°): C(27)–C(28) 1.259(5), N(5)–C(28) 1.071(9), Ag(1)–C(7) 2.058(7), C(29)–C(30) 1.276(5), N(6)–C(30) 1.092(5), Ag(2)–C(22) 2.066(7); N(5)–C(28)–C(27) 178.2(1), C(28)–C(27)–Ag(1) 165.7(6), C(30)–C(29)–Ag(2) 158.9(1), N(3)–C(22)–N(4) 103.3(6), N(6)–C(30)–C(29) 169.1(1), N(1)–C(7)–N(2) 102.8(6). (b) The 1D double-strand supramolecular chains by the π – π interactions and C–H \cdots N hydrogen bonds in **2e**. All hydrogen atoms except those participating in the C–H \cdots N hydrogen bonds, all methyl groups on durennes and all butyl groups on the nitrogen atoms were omitted for clarity.

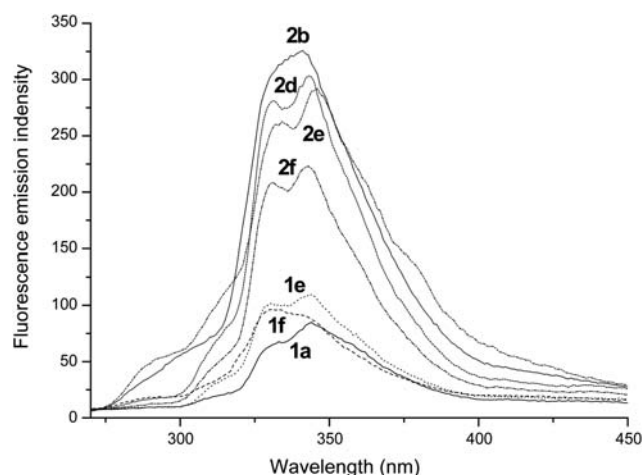


Fig. 10 Emission spectra of **1a** (—), **1e** (···), **1f** (—), **2b** (···), **2d** (···), **2e** (—) and **2f** (···) at 298 K in CH₂Cl₂ (5.0 × 10^{–6} M) solution.

Fluorescent emission spectra of precursors **1a**, **1e** and **1f**, and complexes **2b** and **2d–2f**

As shown in Fig. 10, the fluorescent emission spectra of precursors **1a**, **1e** and **1f** and complexes **2b** and **2d–2f** in dichloromethane at room temperature are obtained upon

excitation at 230 nm (the fluorescent emission spectra of **1b–1d** and **2a** are similar to that of **1a**; the fluorescent emission spectra of **2c**, **2g** and **2h** are similar to that of **2b**). Precursors **1a**, **1e** and **1f** exhibit double emission bands in the region of 330–345 nm, corresponding to intraligand transitions. Complex **2b** exhibits a broad and intense emission band in the region of 325–350 nm. Complexes **2d–2f** show double emission bands in the range of 330–345 nm. The fluorescence emissions of these complexes are stronger than those of their corresponding precursors, which may be assigned to the incorporation of metal–ligand coordination interactions.²⁹ The results show that these metal complexes might be candidates for potential photoactive materials.

Conclusions

In summary, a series of new NHC copper(I), mercury(II) and silver(I) complexes have been synthesized and characterized. Precursor **1e** and complexes **2b–2g** adopt *cis*-conformations, and complexes **2a** and **2h** adopt open *trans*-conformations. Additionally, complexes **2b–2g** possess a macrometallocycle, respectively, formed by a didentate chelate carbene ligand and one/two metal ions. During the preparation of **2d** or **2e**, the acetonitrile are deprotonated in the presence of strong base KO^tBu to form deprotonated acetonitrile ([CHCN]^{2−} for **2d** and [CH₂CN][−] for **2e**). Then the α -carbon atom of deprotonated acetonitrile participates in coordination with metal atoms. In crystal packings, 2D supramolecular layers of **1e**, **2b**, **2c** and **2f–2h**, as well as 1D supramolecular chains of **2d** and **2e** are formed *via* intermolecular weak interactions, including π – π interactions, hydrogen bonds, C–H \cdots π contacts and weak Hg \cdots Br bonds. Further studies on new organometallic compounds from precursors **1a–1f** and analogous ligands are under way.

Experimental

General procedures

Bis(bromomethyl)durene was prepared according to the literature method.³⁰ All manipulations were performed using Schlenk techniques, and solvents were purified by standard procedures. All the reagents for synthesis and analyses were of analytical grade and used without further purification. Melting points were determined with a Boetius Block apparatus. IR spectra were measured on a Bruker IR Equinox-55 infrared spectrophotometer. ¹H and ¹³C{¹H} NMR spectra were recorded on a Varian Mercury Vx 400 spectrometer at 400 MHz and 100 MHz, respectively. Chemical shifts, δ , are reported in ppm relative to the internal standard TMS for both ¹H and ¹³C NMR. *J* values are given in Hz. Elemental analyses were measured using a Perkin-Elmer 2400C Elemental Analyzer. The luminescent spectra were conducted on a Cary Eclipse fluorescence spectrophotometer.

Preparation of dibenzimidazolium (or diimidazolium) salts

Preparation of bis[*N*-(ethyl)benzimidazoliumylmethyl]durene bromide (1a) and bis[*N*-(ethyl)benzimidazoliumylmethyl]durene hexafluorophosphate (1b). A THF solution of benzimidazole (2.000 g, 16.9 mmol) was added to a suspension of oil-free

sodium hydride (0.480 g, 20.3 mmol) in THF (50 mL) and stirred for 1 h at 60 °C. Then THF (40 mL) solution of ethyl bromide (2.029 g, 18.6 mmol) was dropwise added to above solution. The mixture was continued to stir for 48 h at 60 °C, and a yellow solution was obtained. The solvent was removed with a rotary evaporator, and H₂O (100 mL) was added to the residue. Then the solution was extracted with CH₂Cl₂ (3 \times 30 mL), and the extracting solution was dried over anhydrous MgSO₄. After removing CH₂Cl₂, a pale yellow liquid 1-ethylbenzimidazole was obtained. Yield: 2.220 g (90%).

A solution of 1-ethylbenzimidazole (2.013 g, 14.0 mmol) and bis(bromomethyl)durene (2.000 g, 6.25 mmol) in THF (150 mL) was stirred for three days under reflux, and a precipitate was formed. The product was filtered and washed with THF. The white powder of bis[*N*-(ethyl)benzimidazoliumylmethyl]durene bromide (**1a**) was obtained by recrystallization from methanol–diethyl ether. Yield: 3.300 g (86%). Mp: 170–172 °C. Anal. Calcd for C₃₀H₃₆N₄Br₂: C, 58.83; H, 5.92; N, 9.15%. Found: C, 58.66; H, 5.96; N, 9.43%. ¹H NMR (400 MHz, DMSO-*d*₆): δ 1.62 (t, *J* = 7.2, 6H, CH₃), 2.31 (s, 12H, CH₃), 4.84 (q, *J* = 7.2, 4H, CH₂), 5.90 (s, 4H, CH₂), 7.75 (m, 6H, PhH), 8.52 (d, *J* = 8.1, 2H, PhH), 10.40 (s, 2H, 2-bimiH) (bimi: benzimidazole).

NH₄PF₆ (1.171 g, 7.2 mmol) was added to a methanol solution (100 mL) of **1a** (2.000 g, 3.3 mmol) whilst stirring and a white precipitate formed immediately. The product was collected by filtration, washed with small portions of cold methanol, and dried in vacuum to give **1b**. Yield: 1.980 g (82%). Mp: 292–296 °C. Anal. Calcd for C₃₀H₃₆F₁₂N₄P₂: C, 48.52; H, 4.89; N, 7.55%. Found: C, 48.85; H, 5.22; N, 7.81%. ¹H NMR (400 MHz, DMSO-*d*₆): δ 1.66 (t, *J* = 7.2, 6H, CH₃), 2.44 (s, 12H, CH₃), 4.89 (q, *J* = 7.2, 4H, CH₂), 5.95 (s, 4H, CH₂), 7.67 (m, 6H, PhH), 8.55 (d, *J* = 8.3, 2H, PhH), 10.60 (s, 2H, 2-bimiH).

The following dibenzimidazolium (or diimidazolium) salts **1c** and **1e** were prepared in a manner analogous to that for **1a**, and **1d** and **1f** were prepared in a manner analogous to that for **1b**.

Preparation of bis[*N*-(propyl)benzimidazoliumylmethyl]durene chloride (1c). Yield: 4.009 g (84%). Mp: 282–284 °C. Anal. Calcd for C₃₂H₄₀N₄Cl₂: C, 69.26; H, 7.31; N, 10.16%. Found: C, 69.12; H, 7.44; N, 10.52%. ¹H NMR (400 MHz, DMSO-*d*₆): δ 1.65 (t, *J* = 7.2, 6H, CH₃), 1.74 (m, 4H, CH₂), 2.34 (s, 12H, CH₃), 4.84 (t, *J* = 7.2, 4H, CH₂), 5.93 (s, 4H, CH₂), 7.75 (m, 6H, PhH), 8.57 (d, *J* = 8.1, 2H, PhH), 10.43 (s, 2H, 2-bimiH) (bimi: benzimidazole).

Preparation of bis[*N*-(butyl)benzimidazoliumylmethyl]durene iodide (1d). Yield: 1.919 g (80%). Mp: 320–322 °C. Anal. Calcd for C₃₄H₄₄N₄I₂: C, 53.55; H, 5.82; N, 7.35%. Found: C, 53.84; H, 5.48; N, 7.64%. ¹H NMR (400 MHz, DMSO-*d*₆): δ 0.94 (t, *J* = 7.3, 6H, CH₃), 1.44 (m, 4H, CH₂), 1.95 (m, 4H, CH₂), 2.31 (s, 12H, CH₃), 4.85 (t, *J* = 7.3, 4H, CH₂), 5.95 (s, 4H, CH₂), 7.81 (m, 6H, PhH), 8.67 (d, *J* = 8.3, 2H, PhH), 10.41 (s, 2H, 2-bimiH).

Preparation of bis[*N*-(1-pyridinylmethyl)benzimidazoliumylmethyl]durene bromide (1e). Yield: 3.200 g (73%). Mp: 324–326 °C. Anal. Calcd for C₃₈H₃₈N₆Br₂: C, 61.80; H, 5.19; N, 11.38%. Found: 61.44; H, 5.53; N, 11.65%. ¹H NMR (400 MHz, DMSO-*d*₆): δ 2.31 (s, 12H, CH₃), 5.90 (s, 4H, CH₂), 5.94 (s, 4H, CH₂), 7.36 (m, 2H, PhH), 7.66 (m, 6H, PhH), 7.95 (m, 4H, PhH), 8.14 (m, 2H, PhH), 8.42 (d, *J* = 4.8, 2H, PhH), 9.98 (s, 2H, 2-bimiH).

Preparation of bis[*N*-(*n*-butyl)imidazoliumylmethyl]durene hexafluorophosphate (1f**).** Yield: 2.100 g (86%). Mp: 286–288 °C. Anal. Calcd for C₂₆H₄₀F₁₂N₄P₂: C, 44.70; H, 5.77; N, 8.02%. Found: C, 44.71; H, 6.23; N, 7.74%. ¹H NMR (400 MHz, DMSO-*d*₆): δ 0.91 (t, *J* = 5.3, 6H, CH₃), 1.37 (m, 4H, CH₂), 1.86 (t, *J* = 5.3, 4H, CH₂), 2.15 (s, 12H, CH₃), 4.40 (t, *J* = 5.3, 4H, CH₂), 5.83 (s, 4H, CH₂), 7.36 (s, 2H, imiH), 8.58 (s, 2H, imiH), 9.90 (s, 2H, 2-imiH) (imi: imidazole).

Preparation of [durene(CH₂Bimy^{Pr})₂][PdCl₃(DMSO)]₂ (2a**).** A suspension of bis[*N*-(*n*-propyl)benzimidazoliumylmethyl]durene chloride (**1c**) (0.200 g, 0.36 mmol), PdCl₂(CH₃CN)₂ (0.187 g, 0.72 mmol) in acetonitrile (10 mL) and DMSO (5 mL) was refluxed for 24 h. A brown solution was formed, and the acetonitrile were removed with a rotary evaporator. The water (30 mL) was added to the residue, and the solution extracted with CH₂Cl₂ (3 × 20 mL). The extracting solution was dried over anhydrous MgSO₄, then the solution was concentrated to 10 mL and hexane (4 mL) was added. **2a** was obtained as a pale yellow powder. Yield: 0.167 g (57%). Mp: > 320 °C. Anal. Calcd for C₃₆H₅₂Cl₆N₄O₂Pd₂S₂: C, 40.69; H, 4.93; N, 5.27%. Found: C, 40.33; H, 4.72; N, 5.56%. ¹H NMR (400 MHz, DMSO-*d*₆): δ 1.67 (t, *J* = 6.8, 6H, CH₃), 1.74 (m, 4H, CH₂), 2.37 (s, 12H, CH₃), 4.89 (t, *J* = 5.6, 4H, CH₂), 5.96 (s, 4H, CH₂), 7.78 (m, 6H, PhH), 8.60 (d, *J* = 8.1, 2H, PhH), 10.02 (s, 2H, 2-bimiH) (bimi: benzimidazole). ¹³C NMR (100 MHz, DMSO-*d*₆): δ 138.3, 136.2, 132.8, 132.1, 127.1, 126.0 and 125.1 (PhC or imiC), 46.9 (NCH₂Ph), 31.8 (NCH₂C), 17.3 (CCH₂C), 16.8 (PhCH₃), 12.0 (CH₂CH₃).

Preparation of [durene(CH₂BimyEt)₂Cu₂I₂] (2b**).** A suspension of KO^tBu (0.146 g, 1.3 mmol), bis[*N*-(ethyl)benzimidazoliumylmethyl]durene hexafluorophosphate (**1b**) (0.200 g, 0.3 mmol) and copper(i) iodide (0.100 g, 0.5 mmol) in acetonitrile (30 mL) was refluxed for 24 h. A brown solution was formed, and the solvent was removed with a rotary evaporator. The water (30 mL) was added to the residue, and the solution extracted with CH₂Cl₂ (3 × 20 mL). The extracting solution was dried over anhydrous MgSO₄, then the solution was concentrated to 10 mL and hexane (4 mL) was added. As a result, a pale yellow powder was obtained. Yield: 0.126 g (56%). Mp: 352–354 °C. Anal. Calcd for C₃₀H₃₄Cu₂I₂N₄: C, 43.33; H, 4.12; N, 6.74%. Found: C, 43.72; H, 4.50; N, 6.33%. ¹H NMR (400 MHz, DMSO-*d*₆): δ 1.41 (t, *J* = 5.1, 6H, CH₃), 2.36 (s, 12H, CH₃), 4.40 (q, *J* = 5.1, 4H, CH₂), 5.49 (s, 4H, CH₂), 7.49 (m, 4H, PhH), 7.80 (d, *J* = 5.4, 2H, PhH), 8.3 (d, *J* = 5.4, 2H, PhH). ¹³C NMR (100 MHz, DMSO-*d*₆): δ 174.4 (C_{carbene}), 138.2, 135.3, 132.8, 132.0, 127.2, 126.1 and 124.3 (PhC), 47.4 (NCH₂Ph), 32.5 (NCH₂C), 17.1 (PhCH₃), 12.1 (CCH₃).

The following two NHC mercury(II) complexes **2c** and **2d** were prepared in a manner analogous to that for **2b**.

Preparation of [durene(CH₂BimyEt)₂HgBr][0.5[HgBr₄]] (2c**).** Yield: 0.178 g (55%). Mp: 306–308 °C. Anal. Calcd for C₃₀H₃₄Br₃Hg_{1.5}N₄: C, 36.35; H, 3.46; N, 5.65%. Found: C, 36.78; H, 3.74; N, 5.33%. ¹H NMR (400 MHz, DMSO-*d*₆): δ 1.59 (t, *J* = 7.2, 6H, CH₃), 2.27 (s, 12H, CH₃), 4.62 (q, *J* = 7.2, 4H, CH₂), 5.82 (s, 4H, CH₂), 7.72 (s, 4H, PhH), 8.02 (d, *J* = 6.2, 2H, PhH), 8.28 (d, *J* = 6.2, 2H, PhH). ¹³C NMR (100 MHz, DMSO-*d*₆): δ 180.1 (C_{carbene}), 137.2, 135.1, 132.9, 132.0, 131.3, 126.3 and

125.8 (PhC), 46.8 (NCH₂Ph), 33.6 (NCH₂C), 15.1 (PhCH₃), 10.0 (CCH₃).

Preparation of [durene(CH₂benzimy^{Bu})₂Hg₂(CHCN)][HgI₄] (2d**).** Yield: 0.230 g (54%). Mp: 276–278 °C. Anal. Calcd for C₃₆H₄₃Hg₃I₄N₅: C, 26.12; H, 2.62; N, 4.23%. Found: C, 26.57; H, 2.32; N, 4.65%. ¹H NMR (400 MHz, DMSO-*d*₆): δ 0.88 (t, *J* = 7.4, 6H, CH₃), 1.29 (m, 4H, CH₂), 1.83 (m, 4H, CH₂), 2.07 (s, 1H, CH), 2.27 (s, 12H, CH₃), 4.48 (t, *J* = 7.2, 2H, CH₂), 5.81 (s, 2H, CH₂), 7.76 (m, 4H, PhH), 8.12–8.19 (m, 4H, PhH). ¹³C NMR (100 MHz, DMSO-*d*₆): δ 187.3 (C_{carbene}), 137.0, 136.2, 133.2, 132.7, 132.3, 126.3 and 126.0 (PhC), 113.4 (CN), 48.3 (NCH₂Ph), 31.5 (NCH₂C), 30.3 (HgCHHg), 19.2 (CCH₂C), 17.3 (CCH₂C), 16.2 (PhCH₃), 13.4 (CCH₃). IR (KBr): ν CN, 2191 cm⁻¹.

Preparation of [durene(CH₂imy^{Bu})₂Ag₂(CH₂CN)₂] (2e**).** Silver oxide (0.089 g, 0.4 mmol) and KO^tBu (0.146 g, 1.3 mmol) was added to a solution of bis[*N*-(*n*-butyl)imidazoliumylmethyl]durene hexafluorophosphate (**1f**) (0.200 g, 0.3 mmol) in CH₃CN–CH₂Cl₂ (30 mL), and the suspension solution was stirred for 24 h at refluxing. The resulting solution was filtered and concentrated to 10 mL, and Et₂O (5 mL) was added to precipitate a white powder. Isolation by filtration yielded **2e**. Yield: 0.101 g (50%). Mp: 164–166 °C. Anal. Calcd for C₃₀H₄₂Ag₂N₆: C, 51.30; H, 6.03; N, 11.96%. Found: C, 51.71; H, 6.46; N, 11.66%. ¹H NMR (400 MHz, DMSO-*d*₆): δ 0.87 (t, *J* = 7.2, 6H, CH₃), 1.20 (m, 4H, CH₂), 1.70 (m, 4H, CH₂), 2.20 (s, 12H, CH₃), 2.23 (s, 2H, CH₂), 4.01 (t, *J* = 6.0, 4H, CH₂), 5.35 (s, 4H, CH₂), 7.39 (s, 2H, imiH), 7.48 (s, 2H, imiH) (imi: imidazole). ¹³C NMR (100 MHz, DMSO-*d*₆): δ 135.4, 133.0, 123.1 and 122.1 (PhC or imiC), 112.7 (CN), 52.0 (NCH₂CH₂), 50.0 (NCH₂Ph), 33.6 (AgCH₂C), 31.2 (CCH₂C), 19.7 (CCH₂C), 17.4 (PhCH₃), 14.2 (CCH₃). IR (KBr): ν CN, 2166 cm⁻¹. The signal of carbene carbon was not observed.

Preparation of [durene(CH₂BimyPymethyl)₂Ag₂Br₂] (2f**).** Silver oxide (0.070 g, 0.3 mmol) was added to a solution of bis[*N*-(1-pyridinylmethyl)imidazoliumylmethyl]durene bromide (**1e**) (0.200 g, 0.3 mmol) in dichloromethane (30 mL) and the suspension solution was stirred for 24 h at refluxing. The resulting solution was filtered and concentrated to 10 mL, and Et₂O (5 mL) was added to precipitate a white powder. Isolation by filtration yielded **2f**. Yield: 0.156 g (60%). Mp: 288–290 °C. Anal. Calcd for C₃₈H₃₆Ag₂Br₂N₆: C, 47.93; H, 3.81; N, 8.83%. Found: C, 47.58; H, 3.44; N, 8.62%. ¹H NMR (400 MHz, DMSO-*d*₆): δ 2.30 (s, 12H, CH₃), 5.91 (s, 4H, CH₂), 5.95 (s, 4H, CH₂), 7.34 (m, 2H, PhH or PyH), 7.61 (m, 6H, PhH or PyH), 7.92 (m, 4H, PhH or PyH), 8.13 (m, 2H, PhH or PyH), 8.44 (d, *J* = 4.8, 2H, PhH or PyH). ¹³C NMR (100 MHz, DMSO-*d*₆): δ 182.0 (C_{carbene}), 155.8, 150.2, 138.5, 136.2, 133.8, 132.8, 132.1, 124.1, 123.0, 118.9 and 116.8 (PhC or PyC), 50.4 (NCH₂Py), 40.6 (NCH₂Ph), 13.1 (PhCH₃).

The following two NHC silver(I) complexes **2g** and **2h** were prepared in a manner analogous to that for **2f**.

Preparation of [durene(CH₂BimyEt)Ag](PF₆) (2g**).** Yield: 0.098 g (52%). Mp: 256–260 °C. Anal. Calcd for C₃₀H₃₄AgF₆N₄P: C, 51.22; H, 4.87; N, 7.96%. Found: C, 51.61; H, 4.48; N, 7.68%. ¹H NMR (400 MHz, DMSO-*d*₆): δ 1.50 (t, *J* = 5.2, 6H, CH₃), 2.43 (s, 12H, CH₃), 4.46 (q, *J* = 5.2, 4H, CH₂), 5.53 (s, 4H, CH₂), 7.51

Table 4 Summary of crystallographic data for **1e**, **2a** and **2b**

	1e ·CH ₃ CN	2a	2b ·0.5CH ₃ CN
Chemical formula	C ₃₈ H ₃₈ N ₆ ·Br ₂ ·CH ₃ CN	[C ₃₂ H ₄₀ N ₄]·2[PdCl ₃ DMSO]	C ₃₀ H ₃₄ Cu ₂ I ₂ N ₄ ·0.5CH ₃ CN
Fw	779.62	1062.46	852.02
Crystal system	Monoclinic	Triclinic	Triclinic
Space group	<i>P</i> 2 ₁ / <i>c</i>	<i>P</i> 1	<i>P</i> 1
<i>a</i> /Å	14.781(7)	8.885(1)	9.709(1)
<i>b</i> /Å	14.678(7)	10.627(1)	17.216(3)
<i>c</i> /Å	18.540(9)	13.042(1)	19.642(4)
α /°	90	78.793(2)	72.8 (3)
β /°	111.032(1)	80.799(2)	86.3 (3)
γ /°	90	66.276(2)	88.6 (3)
<i>V</i> /Å ³	3754.4(3)	1101.3(2)	3131.2(1)
<i>Z</i>	4	2	2
<i>D</i> _c /Mg m ⁻³	1.379	1.602	1.807
μ /mm ⁻¹	2.197	1.311	3.358
<i>F</i> (000)	1600	538	1668
Crystal size/mm	0.22 × 0.21 × 0.14	0.28 × 0.22 × 0.20	0.14 × 0.12 × 0.10
θ_{\min} , θ_{\max} (°)	1.82, 25.01	2.12, 25.02	1.39, 25.02
<i>T</i> /K	296(2)	296(2)	113(2)
No. of data collected	18 776	5682	10 999
No. of unique data	6616	3868	10 999
No. of refined params	447	240	725
Goodness-of-fit on <i>F</i> ^{2a}	1.032	1.061	1.077
Final <i>R</i> indices ^b [<i>I</i> > 2σ(<i>I</i>)]			
<i>R</i> ₁	0.0405	0.0559	0.0689
<i>wR</i> ₂	0.1205	0.1756	0.1383
<i>R</i> indices (all data)			
<i>R</i> ₁	0.0675	0.0637	0.0921
<i>wR</i> ₂	0.1358	0.1845	0.1524

^a Goof = $[\sum w(F_o^2 - F_c^2)^2/(n - p)]^{1/2}$, where *n* is the number of reflections and *p* is the number of parameters refined. ^b $R_1 = \sum(|F_o| - |F_c|)/\sum|F_o|$; $wR_2 = 1/[\sigma^2(F_o^2) + (0.0691P) + 1.4100P]$ where $P = (F_o^2 + 2F_c^2)/3$.

Table 5 Summary of crystallographic data for **2c–2e**

	2c ·0.5DMSO	2d ·CH ₃ CN	2e
Chemical formula	C ₃₀ H ₃₄ BrHgN ₄ ·0.5HgBr ₄ ·0.5DMSO	C ₃₆ H ₄₃ Hg ₃ I ₄ N ₅ ·CH ₃ CN	C ₃₀ H ₄₂ Ag ₂ N ₆
Fw	1030.29	1696.18	702.43
Crystal system	Triclinic	Triclinic	Triclinic
Space group	<i>P</i> 1	<i>P</i> 1	<i>P</i> 1
<i>a</i> /Å	14.017(1)	12.212(8)	10.950(6)
<i>b</i> /Å	16.221(2)	13.311(8)	14.822 (7)
<i>c</i> /Å	18.554(2)	16.692(1)	19.4 (9)
α /°	89.7 (2)	71.1 (1)	98.1 (1)
β /°	69.7 (2)	75.7 (1)	95.9 (1)
γ /°	72.1 (2)	62.9 (1)	107.0 (1)
<i>V</i> /Å ³	3745.0(8)	2271.9(2)	2955.6(3)
<i>Z</i>	2	2	2
<i>D</i> _c /Mg m ⁻³	1.826	2.479	1.579
μ /mm ⁻¹	9.403	12.862	1.355
<i>F</i> (000)	1950	1536	1432
Crystal size/mm	0.24 × 0.20 × 0.16	0.24 × 0.20 × 0.18	0.28 × 0.26 × 0.20
θ_{\min} , θ_{\max} (°)	1.63, 26.00	1.77, 25.03	1.07, 25.03
<i>T</i> /K	296(2)	296(2)	296(2)
No. of data collected	14 562	11 724	15 297
No. of unique data	14 562	7972	10 382
No. of refined params	783	466	690
Goodness-of-fit on <i>F</i> ^{2a}	1.029	1.030	1.020
Final <i>R</i> indices ^b [<i>I</i> > 2σ(<i>I</i>)]			
<i>R</i> ₁	0.0412	0.0383	0.0488
<i>wR</i> ₂	0.1001	0.0978	0.1413
<i>R</i> indices (all data)			
<i>R</i> ₁	0.0657	0.0481	0.0823
<i>wR</i> ₂	0.1063	0.1043	0.1698

^a Goof = $[\sum w(F_o^2 - F_c^2)^2/(n - p)]^{1/2}$, where *n* is the number of reflections and *p* is the number of parameters refined. ^b $R_1 = \sum(|F_o| - |F_c|)/\sum|F_o|$; $wR_2 = 1/[\sigma^2(F_o^2) + (0.0691P) + 1.4100P]$ where $P = (F_o^2 + 2F_c^2)/3$.

Table 6 Summary of crystallographic data for **2f–2h**

	2f ·DMSO	2g ·0.5H ₂ O	2h
Chemical formula	C ₃₈ H ₃₆ Ag ₂ Br ₂ N ₆ ·DMSO	C ₃₀ H ₃₄ AgN ₄ ·PF ₆ ·0.5H ₂ O	C ₃₄ H _{43.88} Ag ₂ I _{0.1} N ₄ O _{1.88}
Fw	1030.42	712.46	768.56
Crystal system	Triclinic	Triclinic	Monoclinic
Space group	<i>P</i> 1	<i>P</i> 1	<i>C</i> ₂ / <i>c</i>
<i>a</i> /Å	10.097(2)	9.368(1)	3.133(4)
<i>b</i> /Å	13.533(3)	13.897(2)	18.772(4)
<i>c</i> /Å	15.4 (3)	14.595(2)	20.002(2)
α /°	104.0 (3)	103.6 (2)	90
β /°	97.6 (3)	102.9 (2)	15.8 (5)
γ /°	94.5 (4)	104.9 (2)	90
<i>V</i> /Å ³	2010.4(7)	1699.1(4)	3784.7(2)
<i>Z</i>	2	2	4
<i>D</i> _c /Mg m ^{−3}	1.699	1.393	1.349
μ /mm ^{−1}	3.051	0.699	1.155
<i>F</i> (000)	1024	726	1563
Crystal size/mm	0.28 × 0.22 × 0.20	0.34 × 0.32 × 0.30	0.22 × 0.20 × 0.18
θ_{\min} , θ_{\max} (°)	1.56, 25.03	2.38, 25.01	1.94, 25.01
<i>T</i> /K	296(2)	296(2)	296(2)
No. of data collected	10 282	8589	3344
No. of unique data	7035	5920	3344
No. of refined params	510	431	197
Goodness-of-fit on <i>F</i> ² _o	1.032	1.071	1.150
Final <i>R</i> indices ^b [<i>I</i> > 2σ(<i>I</i>)]			
<i>R</i> ₁	0.0357	0.0473	0.0352
<i>wR</i> ₂	0.0962	0.1486	0.1164
<i>R</i> indices (all data)			
<i>R</i> ₁	0.0525	0.0543	0.0400
<i>wR</i> ₂	0.1072	0.1573	0.1192

^a Goof = $[\sum w(F_o^2 - F_c^2)^2/(n - p)]^{1/2}$, where *n* is the number of reflections and *p* is the number of parameters refined. ^b $R_1 = \sum(|F_o| - |F_c|)/\sum|F_o|$; $wR_2 = 1/[\sigma^2(F_o^2) + (0.0691P) + 1.4100P]$ where $P = (F_o^2 + 2F_c^2)/3$.

(m, 4H, PhH), 7.84 (d, *J* = 5.5, 2H, PhH), 8.33 (d, *J* = 5.5, 2H, PhH). ¹³C NMR (100 MHz, DMSO-*d*₆): δ 175.0 (C_{carbene}), 138.3, 133.1, 128.4, 118.1 and 112.2 (PhC), 50.1 (NCH₂Ph), 48.2 (NCH₂C), 14.8 (PhCH₃), 10.8 (CCH₃).

Preparation of [durene(CH₂BimyⁿBu)₂Ag₂(OH)₂] (2h). Yield: 0.146 g (50%). Mp: 150–152 °C. Anal. Calcd for C₃₄H_{43.88}I_{0.1}N₄O_{1.88}Ag₂: C, 53.23; H, 5.77; N, 7.30%. Found: C, 53.67; H, 5.32; N, 7.72%. ¹H NMR (400 MHz, DMSO-*d*₆): δ 0.92 (t, *J* = 7.0, 6H, CH₃), 1.37 (m, 4H, CH₂), 1.87 (m, 4H, CH₂), 2.19 (s, 12H, CH₃), 4.44 (t, *J* = 7.0, 4H, CH₂), 5.57 (s, 4H, CH₂), 7.56 (m, 4H, PhH), 7.86 (d, *J* = 7.8, 2H, PhH), 8.13 (d, *J* = 7.8, 2H, PhH). ¹³C NMR (100 MHz, DMSO-*d*₆): δ 181.3 (C_{carbene}), 138.3, 133.1, 129.4, 119.9 and 115.3 (PhC), 53.2 (NCH₂Ph), 48.3 (NCH₂C), 33.7 (CCH₂C), 25.6 (CCH₂C), 14.2 (CCH₃), 9.2 (PhCH₃).

X-Ray structure determinations†

For complexes **2a–2h**, selected single crystals were mounted on a Bruker APEX II CCD diffractometer at 293(2) K with Mo-*K* α radiation (λ = 0.71073 Å) by ω scan mode. Data collection and reduction were performed using the SMART and SAINT software³¹ with frames of 0.6° oscillation in the range of 1.8° < θ < 25°. An empirical absorption correction was applied using the SADABS program.³² The structures were solved by direct methods and all non-hydrogen atoms were subjected to anisotropic refinement by full-matrix least squares on *F*² using the SHELXTL package.³³ All hydrogen atoms were generated

geometrically (C–H bond lengths fixed at 0.96 Å), assigned appropriated isotropic thermal parameters and included in the final calculations. Crystallographic data are summarized in Tables 4–Table 6 for **1e** and **2a–2h**.

Acknowledgements

This work was financially supported by the National Science Foundation of China (Project Grant No. 20872111) and the Natural Science Foundation of Tianjin (07JCYBJC00300).

References

- 1 A. J. Arduengo III, R. L. Harlow and M. Kline, *J. Am. Chem. Soc.*, 1991, **113**, 361–363.
- 2 (a) F. E. Hahn and M. C. Jahnke, *Angew. Chem., Int. Ed.*, 2008, **47**, 3122–3172; (b) P. L. Arnold and I. J. Casely, *Chem. Rev.*, 2009, **109**, 3599–3611; (c) F. E. Hahn, M. C. Jahnke and T. Pape, *Organometallics*, 2007, **26**, 150–154.
- 3 (a) F. E. Hahn, L. Wittenbecher, D. Le Van and R. Frohlich, *Angew. Chem., Int. Ed.*, 2000, **39**, 541–544; (b) F. E. Hahn, T. von Fehren and T. Lügger, *Inorg. Chim. Acta*, 2005, **358**, 4137–4144; (c) F. E. Hahn and M. Foth, *J. Organomet. Chem.*, 1999, **585**, 241–245; (d) S. C. Zinner, C. F. Rentzsch, E. Herdtweck, W. A. Herrmann and F. E. Kühn, *Dalton Trans.*, 2009, 7055–7062.
- 4 (a) M. Poyatos, J. A. Mata and E. Peris, *Chem. Rev.*, 2009, **109**, 3677–3707; (b) L. H. Gade and S. B. Laponnaz, *Coord. Chem. Rev.*, 2007, **251**, 718–725; (c) W. J. Sommer and M. Weck, *Coord. Chem. Rev.*, 2007, **251**, 860–873.
- 5 (a) J. C. Y. Lin, R. T. W. Huang, C. S. Lee, A. Bhattacharyya, W. S. Huang and I. J. B. Lin, *Chem. Rev.*, 2009, **109**, 3561–3598; (b) S. Gischig and A. Togni, *Organometallics*, 2005, **24**, 203–205; (c)

- B. S. Khalid, M. Yasumasa, Y. Ken-ichi and T. Kiyoshi, *Angew. Chem., Int. Ed.*, 2009, **48**, 8733–8735.
- 6 (a) K. M. Lee, J. C. C. Chen, C. J. Huang and I. J. B. Lin, *CrystEngComm*, 2007, **9**, 278–281; (b) U. J. Scheele, S. Dechert and F. Meyer, *Inorg. Chim. Acta*, 2006, **359**, 4891–4900; (c) Q. X. Liu, L. N. Yin and J. C. Feng, *J. Organomet. Chem.*, 2007, **692**, 3655–3663.
- 7 (a) J. C. Garrison and W. J. Youngs, *Chem. Rev.*, 2005, **105**, 3978–4008; (b) F. E. Hahn, M. C. Jahnke and T. Pape, *Organometallics*, 2006, **25**, 5927–5936; (c) M. C. Jahnke, J. Paley, F. Hupka, J. J. Weigand and F. E. Hahn, *Z. Naturforsch.*, 2009, **64b**, 1458–1462.
- 8 (a) J. J. Van Veldhuizen, J. E. Campbell, R. E. Giudici and A. H. Hoveyda, *J. Am. Chem. Soc.*, 2005, **127**, 6877–6882; (b) K. S. Coleman, H. T. Chamberlayne, S. Turberville, M. L. H. Green and A. R. Cowley, *Dalton Trans.*, 2003, 2917–2922; (c) W. A. Herrmann, S. K. Schneider, K. Öfele, M. Sakamoto and E. Herdtweck, *J. Organomet. Chem.*, 2004, **689**, 2441–2444.
- 9 (a) M. C. Perry, X. H. Cui and K. Burgess, *Tetrahedron: Asymmetry*, 2002, **13**, 1969–1972; (b) L. G. Bonnet, R. E. Douthwaite and R. Hodgson, *Organometallics*, 2003, **22**, 4384–4386; (c) C. Marshall, M. F. Ward and W. T. A. Harrison, *J. Organomet. Chem.*, 2005, **690**, 3970–3975; (d) H. Clavier, J. C. Guillemin and M. Mauduit, *Chirality*, 2007, **19**, 471–476; (e) M. S. Jeletic, I. Ghiviriga, K. A. Abboud and A. S. Veige, *Organometallics*, 2007, **26**, 5267–5270.
- 10 (a) C. M. Zhang and M. L. Trudell, *Tetrahedron Lett.*, 2000, **41**, 595–598; (b) D. S. Clyne, J. Jin, E. Genest, J. C. Gallucci and T. V. RajanBabu, *Org. Lett.*, 2000, **2**, 1125–1128; (c) A. A. Danopoulos, A. A. D. Tulloch, S. Winston, G. Eastham and M. B. Hursthouse, *J. Chem. Soc., Dalton Trans.*, 2003, 1009–1015; (d) W. L. Duan, M. Shi and G. B. Rong, *Chem. Commun.*, 2003, 2916–2917; (e) A. R. Chianese and R. H. Crabtree, *Organometallics*, 2005, **24**, 4432–4436; (f) W. F. Wang, F. J. Wang and M. Shi, *Organometallics*, 2010, **29**, 928–933; (g) B. P. Morgan, G. A. Galdamez, R. J. Gilliard Jr. and R. C. Smith, *Dalton Trans.*, 2009, 2020–2028.
- 11 (a) D. H. Brown, G. L. Nealon, P. V. Simpson, B. W. Skelton and Z. Wang, *Organometallics*, 2009, **28**, 1965–1968; (b) A. T. Normand and K. J. Cavell, *Eur. J. Inorg. Chem.*, 2008, 2781–2800; (c) B. Liu, W. Chen and S. Jin, *Organometallics*, 2007, **26**, 3660–3667; (d) D. Pugh, J. A. Wright, S. Freeman and A. A. Danopoulos, *Dalton Trans.*, 2006, 775–782; (e) F. E. Hahn, M. C. Jahnke and T. Pape, *Organometallics*, 2007, **26**, 150–154.
- 12 (a) D. J. Nielsen, K. J. Cavell, B. W. Skelton and A. H. White, *Organometallics*, 2006, **25**, 4850–4856; (b) A. A. D. Tulloch, A. A. Danopoulos, G. J. Tizzard, S. J. Coles, M. B. Hursthouse, R. S. Hay-Motherwell and W. B. Motherwell, *Chem. Commun.*, 2001, 1270–1271; (c) D. J. Nielsen, K. J. Cavell, B. W. Skelton and A. H. White, *Inorg. Chim. Acta*, 2002, **327**, 116–125; (d) X. Q. Zhang, Y. P. Qiu, B. R. and M. M. Luo, *Organometallics*, 2009, **28**, 3093–3099.
- 13 (a) Q. X. Liu, X. J. Zhao, X. M. Wu, J. H. Guo and X. G. Wang, *J. Organomet. Chem.*, 2007, **692**, 5671–5679; (b) Q. X. Liu, X. Q. Yang, X. J. Zhao, S. S. Ge, S. W. Liu, Y. Zang, H. B. Song, J. H. Guo and X. G. Wang, *CrystEngComm*, DOI: 10.1039/b919007d.
- 14 A. A. D. Tulloch, A. A. Danopoulos, S. Winston, S. Kleinhenz and G. Eastham, *J. Chem. Soc., Dalton Trans.*, 2000, 4499–4506.
- 15 (a) I. B. Michael, T. W. Hambley, R. S. Michael and A. G. Swincer, *Organometallics*, 1985, **4**, 494–500; (b) Y. Han and H. V. Huynh, *Dalton Trans.*, 2009, 2201–2209.
- 16 L. Rajput and K. Biradha, *CrystEngComm*, 2009, **11**, 1220–1222.
- 17 C. A. Ellis, M. A. Miller, J. Spencer, J. Z. Schpectorc and E. R. T. Tiekink, *CrystEngComm*, 2009, **11**, 1352–1361.
- 18 X. P. Zhou, S. H. Lin, D. Li and Y. G. Yin, *CrystEngComm*, 2009, **11**, 1899–1903.
- 19 J. Ramos, V. M. Yartsev, S. Golhen, L. Ouahab and P. Delhaes, *J. Mater. Chem.*, 1997, **7**, 1313–1319.
- 20 G. Mahmoudi and A. Morsali, *CrystEngComm*, 2007, **9**, 1062–1072.
- 21 (a) S. Inoue and Y. Sato, *Organometallics*, 1986, **5**, 1197–1201; (b) P. S. Pregosin, *Inorg. Chim. Acta*, 1980, **45**, L7–L9; (c) M. Robert, F. George, A. J. McAlees, M. Parvez and P. J. Roberts, *J. Chem. Soc., Dalton Trans.*, 1982, 1699–1708; (d) B. Luigi, B. Silvia, Z. Valerio, A. G. Vincenzo and B. Dario, *New J. Chem.*, 1992, **16**, 693–696; (e) H. William and G. O. Allen, *Acta Cryst.*, 1999, **55**, 1406–1408.
- 22 (a) F. E. Hahn, C. Radloff, T. Pape and A. Hepp, *Chem.–Eur. J.*, 2008, **14**, 10900–10904; (b) A. Rit, T. Pape and F. E. Hahn, *J. Am. Chem. Soc.*, 2010, **132**, 4572–4573.
- 23 Z. X. Lian, J. W. Cai, C. H. Chen and H. B. Luo, *CrystEngComm*, 2007, **9**, 319–327.
- 24 R. P. A. Bettens, D. Dakternieks, A. Duthie, F. S. Kuan and E. R. T. Tiekink, *CrystEngComm*, 2009, **11**, pp. 1362–1372.
- 25 L. H. Zhao, Y. P. Quan, A. H. Yang, J. Z. Cui, H. L. Gao, F. L. Lu, W. Shi and P. Cheng, *CrystEngComm*, 2009, **11**, 1427–1432.
- 26 M. L. Cole and P. C. Junk, *CrystEngComm*, 2004, **6**, 173–176.
- 27 F. Neve and A. Crispini, *CrystEngComm*, 2003, **5**, 265–268.
- 28 S. F. Alshahateet, R. Bishop, D. C. Craig and M. L. Scudder, *CrystEngComm*, 2001, **48**, 1–5.
- 29 (a) F. J. B. dit Dominique, H. Gornitzka, A. Sournia-Saquet and C. Hemmert, *Dalton Trans.*, 2009, 340–352; (b) X. X. Zhao, J. P. Ma, D. Z. Shen, Y. B. Dong and R. Q. Huang, *CrystEngComm*, 2009, **11**, 1281–1290.
- 30 A. W. vander Made and R. H. vander Made, *J. Org. Chem.*, 1993, **58**, 1262–1263.
- 31 *SMART 5.0 and SAINT 4.0 for Windows NT, Area Detector Control and Integration Software*, Bruker Analytical X-Ray Systems, Inc., Madison, WI, USA, 1998.
- 32 G. M. Sheldrick, *SADABS, Program for Empirical Absorption Correction of Area Detector Data*, Univ. of Göttingen, Germany, 1996.
- 33 G. M. Sheldrick, *SHELXTL 5.10 for Windows NT, Structure Determination Software*, Bruker Analytical X-Ray Systems, Inc., Madison, WI, USA, 1997.